

Supporting Information

Non-Adiabatic Reaction Dynamics in the Gas-Phase Formation of Phosphinidenesilylene (HPSi) – The Isovalent Counterpart of Hydrogen Isocyanide (HNC) - Under Single-Collision Conditions

Chao He,^a Zhenghai Yang,^a Srinivas Doddipatla,^a Long Zhao,^a Shane Goettl,^a Ralf I. Kaiser^{a*}

^a *Department of Chemistry, University of Hawai'i at Manoa, Honolulu, Hawaii 96822, USA*

Corresponding Author Prof. Dr. Ralf I. Kaiser: ralfk@hawaii.edu

Mateus Xavier Silva,^b Breno R. L. Galvão^{b*}

^b *Centro Federal de Educação Tecnológica de Minas Gerais, CEFET-MG, Av. Amazonas 5253,
30421-169 Belo Horizonte, Minas Gerais, Brazil*

Corresponding Author Prof. Dr. Breno R L Galvão: brenogalvao@gmail.com

1. Experimental and Computational

Experimental: The gas-phase reaction of atomic silicon (Si; ^3P) with phosphine (PH_3 ; X^1A_1) was studied under single-collision conditions using a universal crossed molecular beams machine at the University of Hawaii.¹ In the primary source chamber, a pulsed supersonic beam of ground state silicon atoms was prepared *in situ* by ablation of silicon from a rotating silicon rod at 266 nm (Nd:YAG laser; 5 ± 1 mJ per pulse; 30Hz)² and seeding the ablated atoms in neon gas (Ne; 99.999%; Specialty Gases of America). The neon-seeded beam of silicon atoms was skimmed and velocity-selected by a four-slot chopper wheel yielding a peak velocity v_p of 947 ± 17 m s⁻¹ and speed ratio S of 6.8 ± 0.4 (Table S1). Laser-induced fluorescence interrogation of neon-seeded silicon beam indicates that all silicon atoms are in their electronic ground state (^3P).³ In the secondary source chamber, the supersonic beam of phosphine ($\geq 99.9995\%$; Matheson Tri-Gas), which was regulated at 550 Torr with $v_p = 805 \pm 9$ m s⁻¹ and $S = 12.4 \pm 0.1$ (Table S1), crossed perpendicularly with the primary beam silicon atoms in the main chamber leading to a collision energy (E_C) of (11.9 ± 0.2) kJ mol⁻¹ and a center of mass angle (Θ_{CM}) of $(45.9 \pm 0.5)^\circ$. The neutral reaction products entering the detector were ionized by electron impact ionizer (80 eV),⁴ then filtered according to the mass-to-charge ratio (m/z) utilizing a quadrupole mass spectrometer (QMS, Extrel, QC 150), and eventually recorded by a Daly-type ion counter.⁵ The detector is housed within a triply differentially pumped and rotatable chamber that allows the collection of angularly-resolved time-of-flight (TOF) spectra in the plane defined by both reactant beams. To obtain the information on the reaction dynamics, a forward-convolution method was used to transform the laboratory frame (LAB) data into the center of mass frame (CM),⁶⁻⁷ which represents an iterative method whereby user-defined CM translational energy $P(E_T)$ and angular $T(\theta)$ flux distributions are varied iteratively until a best fit of the laboratory-frame TOF spectra and angular distributions are achieved. These functions comprise the reactive differential cross-section $I(\theta, u)$, which is taken to be separable into its CM scattering angle θ and CM velocity u components, $I(u, \theta) \sim P(u) \times T(\theta)$. The error ranges of the $P(E_T)$ and $T(\theta)$ functions are determined within the 1σ limits of the corresponding laboratory angular distribution and beam parameters (beam spreads, beam velocities) while maintaining a good fit of the laboratory TOF spectra.

Computational:

The electronic structure calculations reported in this work were performed using the GAMESS-US⁸ and MOLPRO⁹ packages. First, density functional theory (DFT)¹⁰ calculations employing the M06-2X¹¹ exchange and correlation functional were used along with the cc-pV(T+d)Z basis set¹²⁻¹⁴. Note that the functional chosen is documented to perform better than conventional and widely used ones for barrier heights (both hydrogen-transfer and non-hydrogen-transfer), with mean errors around 5 kJ mol⁻¹.¹⁵ For the specific chemical elements explored in this work, such calculations for the P-H and Si-H bond energy in PH₃ and SiH₄ agree with the experimental values¹⁶⁻¹⁷ within 8 and 9 kJ mol⁻¹ (respectively). All calculations employ restricted wavefunctions in order to avoid spin contamination. Vibrational analyses were carried out for all stationary points found within the M06-2X/cc-pV(T+d)Z approach. Structures that corresponded to energy minima were confirmed by presenting only real vibrational frequencies, while transition states (TSs) were confirmed by the presence of a single imaginary frequency. Intrinsic reaction coordinate (IRC) calculations starting from each TS were performed to ensure the correct connection paths. The reported energies of all structures are always zero-point energy (ZPE) corrected and no symmetry restrictions were imposed in any calculation.

Singlet/triplet crossings

A search for the lowest energy on the seam of intersections between singlet and triplet electronic potential energy surfaces was also carried out with the M06-2X/cc-pV(T+d)Z method without any constraints and yielded two different minimum energy crossing points (MSXs). The MSXs are not conventional stationary structures on the potential energy surface, and to perform ZPE corrections for these cases, a different procedure is performed. First, we calculate the conventional Hessian matrix for both singlet and triplet states independently at the MSX geometry. After that, the coordinate perpendicular to the seam must be projected out (along with the rotational and translational degrees of freedom) to generate a new effective Hessian matrix as described in Refs.¹⁸⁻²⁰. The new effective Hessian matrix is then diagonalized to provide the 3N-7 vibrational frequencies of the MSX, using the implementation described in Ref.²¹. These final frequencies are used for ZPE corrections of the MSX energies.

The probabilities of singlet-triplet transitions depend on the magnitude of the spin-orbit coupling (SOC). To calculate this, we have used the full valence complete active space self-consistent

field (CASSCF) method with the aug-cc-pV(Q+d)Z basis set. After reoptimization of the crossing point, the full spin-orbit matrix was calculated with the Breit-Pauli operator²² as implemented in MOLPRO. The spin-free electronic Hamiltonian eigenstates, $|S\rangle$, $|T, 1\rangle$, $|T, 0\rangle$, and $|T, -1\rangle$, are employed to build the total Hamiltonian matrix representation ($H_{el} + H_{SO}$). The magnitude of the V_{SO} term is then calculated from the matrix elements as:

$$V_{SO}^2 = \sum_{M_S=-1}^1 |\langle T, M_S | H_{SO} | S \rangle|^2.$$

Energy refinement and multireference character

To further improve the accuracy of our results, we have performed single point energy calculations at the CCSD(T)-F12/aug-cc-pV(T+d)Z²³⁻²⁴ level in all geometries optimized at the M06-2X/cc-pV(T+d)Z level, and we report these energies in the manuscript, which are abbreviated as CCSD(T)-F12/aug-cc-pV(T+d)Z//M06-2X/cc-pV(T+d)Z+ZPE(M06-2X/cc-pV(T+d)Z). From the CCSD(T)-F12 calculations, we could also extract the T1²⁵ diagnostic to check if some of the reported structures had a higher than usual multireference (MR) character. The values are given in Table S3, from where it can be seen that most structures show $T1 < 0.03$, for which cases the MR character should not be a serious problem. The exceptions are **p4**, the transition states from **T_{2a}** to **p3**, and **T_{2a}** to **p4** (both of which are too high in energy to be relevant for the experimental conditions), and from **S₂** to **p2**, and **S₂** to **S₃**.

To address the possibility of an inaccurate result caused by MR character, we tackle the problem in two ways. First, we repeated all the geometry optimizations and frequency calculations using a DFT functional with better performance for MR structures (and less HF exchange), for which case we choose the M06 functional, which is known to perform about 2.4 times better¹⁰ than M06-2X for systems with a strong MR character. The results are given in Figure S2, in which the values for both M06-2X and M06 are given together. As can be seen, both functionals have an overall good agreement regarding the possible reaction mechanisms, and their deviations in cases with a larger T1 diagnostic is within the expected accuracy of a DFT calculation.

Secondly, for the cases with a larger T₁ diagnostic with possible consequences for the interpretation of the experiments, we have performed accurate multi-reference calculations to make sure all the conclusions are correct. Their geometry were first optimized at the full valence

CASSCF level with the aug-cc-pV(Q+d)Z basis set, followed by a ZPE calculation. At the optimized geometries we have refined the energy values by performing a multireference configuration interaction calculation including the Davidson correction, MRCI(Q), also with the aug-cc-pV(Q+d)Z basis set. The energy of the transition states from S_2 to **p2** and from S_2 to S_3 , are relevant to the final product distribution and have significant MR character, and we therefore compare the M06-2X, M06, CCSD(T)-F12 and MRCI(Q) results (calculated as described above). As the relevant parameter for the RRKM calculations is the energy difference between the TS and the S_2 minimum, we report below the energies with respect to S_2 in kJ mol^{-1} .

	MRCI(Q)	CCSD(T)-F12	M06-2X	M06
S_2 - S_3	103	111	114	104
S_2 - p2	180	193	183	180

Considering that the MRCI energy is not exact and still may show a 4 kJ mol^{-1} error, the results are in a fairly good agreement, in spite of the T_1 diagnostic, and therefore we believe that the interpretation of the experiments throughout the manuscript is correct.

Finally, the T_1 diagnostic of the triplet state of the HPSi molecule (**p4**) was 0.034, and it can be seen from Figure S2 that the M06 functional predicts that triplet HSiP (**p3**) is slightly lower than **p4**, while M06-2X predicts them as nearly degenerate. Even though this product was not observed experimentally in this work, it is worth predicting an accurate value for its energy at the MRCI(Q) level. With this, we found that HSiP is indeed 15 kJ mol^{-1} lower in energy than HPSi, which agrees well with the difference of 19 kJ mol^{-1} at the CCSD(T)-F12 level reported in the Figure 3 of the manuscript.

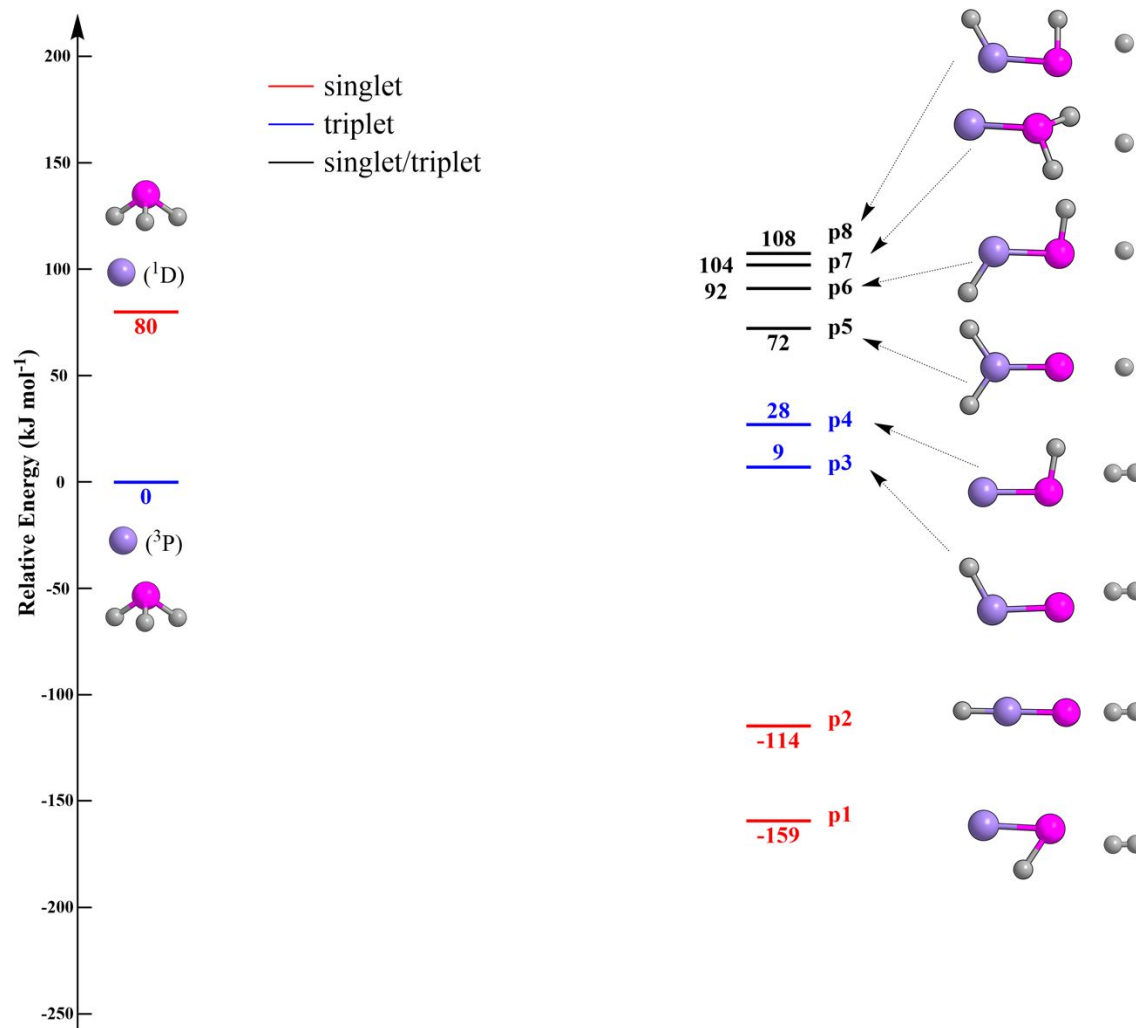


Figure S1. Schematic representation of reactants and products of the reaction of atomic silicon (Si; ³P/¹D) with phosphine (PH₃; X¹A₁) leading to **p1** - **p8**. Energies calculated at the CCSD(T)-F12/aug-cc-pV(T+d)Z//M06-2X/cc-pV(T+d)Z+ZPE(M06-2X/cc-pV(T+d)Z) level are shown in kJ mol⁻¹ and are relative to the energy of the separated reactants. Atoms are colored as follows: silicon (purple); hydrogen (gray); phosphorus (pink).

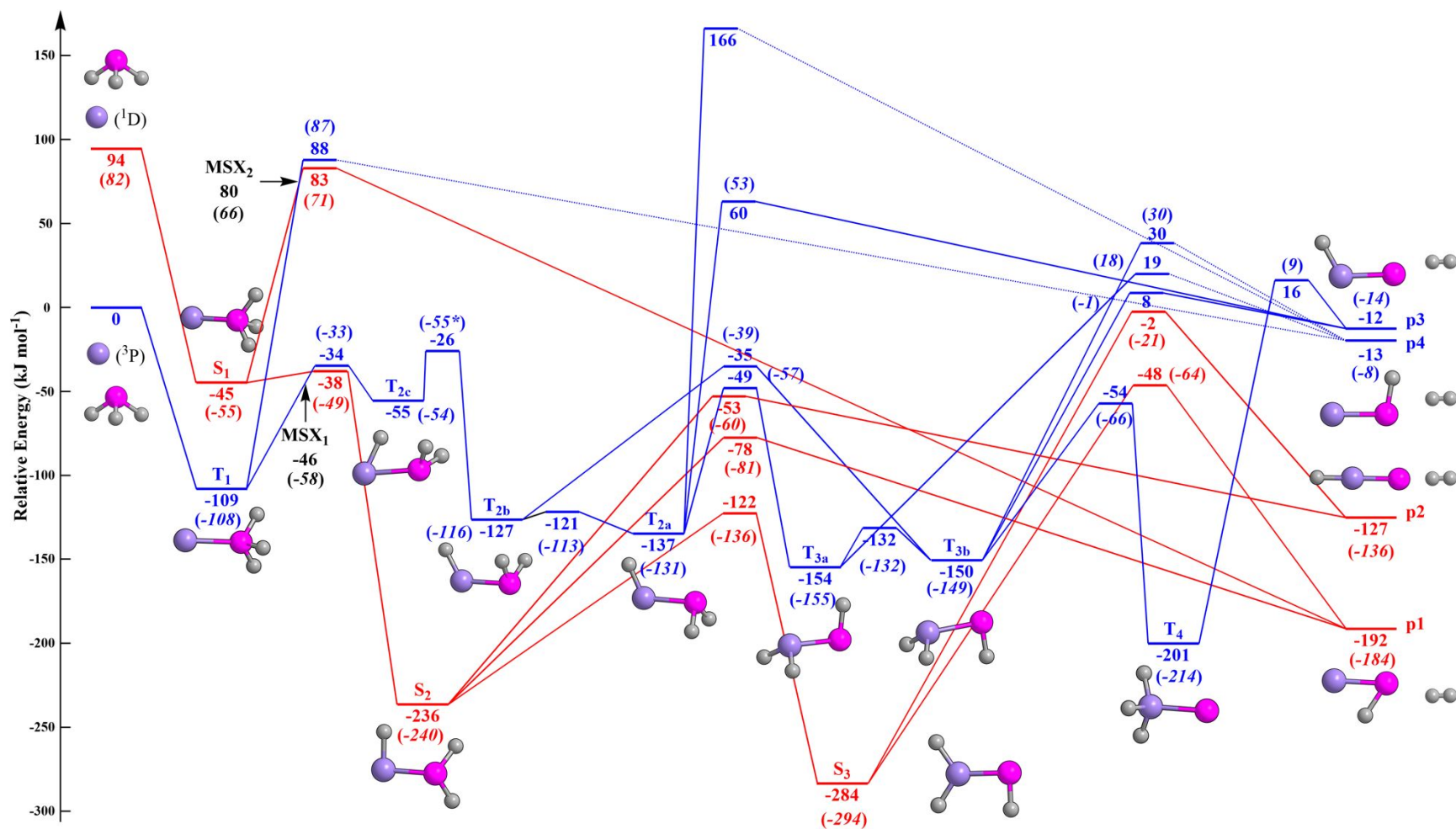


Figure S2. Schematic representation of the potential energy surface of the reaction of atomic silicon (Si; ³P/¹D) with phosphine (PH₃; X¹A₁). The plain numbers give the energies at the M06-2X/cc-pV(T+d)Z level, and those under parenthesis refer to M06/cc-pV(T+d)Z calculations. All results are zero-point energy corrected. The asterisk indicates that, although the T_{2c}-T_{2b} TS seem degenerate with the T_{2c} minimum at the M06 level, the ZPE uncorrected energy shows a true TS slightly above T_{2c} with a single imaginary frequency. Atoms are colored as follows: silicon (purple); hydrogen (gray); phosphorus (pink).

Table S1. Peak velocities (v_p) and speed ratios (S) of the silicon (Si), and phosphine (PH₃) beams along with the corresponding collision energy (E_C) and center-of-mass angle (Θ_{CM}).

Beam	v_p (m s ⁻¹)	S	E_C (kJ mol ⁻¹)	Θ_{CM} (degree)
Si(³ P)	947 ± 17	6.8 ± 0.4		
PH ₃ (X ¹ A ₁)	805 ± 9	12.4 ± 0.1	11.9 ± 0.2	45.9 ± 0.5

Table S2. Statistical branching ratios (%) for the reaction of the silicon atom (Si; ³P) with phosphine (PH₃; X¹A₁). Here, **p1** and **p2** denote singlet phosphinidenesilylene (HPSi; X¹A') and singlet silylidynephosphine (HSiP; X¹Σ⁺), respectively.

E_C (kJ mol ⁻¹)	S₂ → p1	S₃ → p1	S₂ → p2	S₃ → p2
0	62.29	11.86	25.84	0.01
11.9	53.39	13.11	33.46	0.04

Table S3. Optimized Cartesian coordinates and vibrational frequencies for all intermediates, transition states, minima-on-the-seam-of-crossings (MSX), reactants, and products involved in the reactions of the atomic silicon (Si; $^3P/{}^1D$) with phosphine (PH₃; X^1A_1).

Reagents

PH₃; C_{3v}; X¹A₁

P	0.0657489556	-0.0000001858	-0.0019137497
H	-0.7320439127	0.0000003515	1.1624302654
H	-0.6826538144	1.0274840772	-0.6156228017
H	-0.6826536606	-1.0274842429	-0.6156233055

Frequencies

1020.828
 1156.119
 1156.576
 2457.598
 2460.576
 2462.354

T1 diagnostic: 0.01428312

Products

H₂

H	0.0000000000	0.0000000000	0.3694968462
H	0.0000000000	0.0000000000	-0.3694968462

Frequencies

4464.920

T1 diagnostic: 0.00594717

HPSi – triplet; C_s; $^3A''$

P	0.0000000000	-0.0488355711	-1.0502786731
Si	0.0000000000	0.0053951945	1.2049906034
H	0.0000000000	1.3503725664	-1.3013513088

Frequencies

445.27
686.35
2368.55

T1 diagnostic: 0.03382185

HSiP – triplet; $C_s; {}^3A'$

Si	0.0000000000	-0.0630418847	-1.0618623751
P	0.0000000000	0.0156022102	1.0204344861
H	0.0000000000	1.2442727099	-1.7971643838

Frequencies

552.801
620.114
2123.135

T1 diagnostic: 0.02753003

HSiP – singlet; $C_{\infty v}; {}^1\Sigma^+$

Si	0.0000000000	0.0000000000	-0.9730704991
P	0.0000000000	0.0000000000	0.9630601956
H	0.0000000000	0.0000000000	-2.4454507659

Frequencies

330.88
331.03
778.15
2296.63

T1 diagnostic: 0.02204396

HPSi – singlet; $C_s; {}^1A'$

Si	0.0000000000	0.0180207923	-1.0744441180
----	--------------	--------------	---------------

H	0.0000000000	-1.2593728551	0.2117421948
P	0.0000000000	0.0262746117	0.9665566538

Frequencies

673.503
885.731
2013.335

T1 diagnostic: 0.01911852

c-HSiPH

Si	-0.0002891442	0.0599311195	-1.0656052695
H	0.0003978713	-1.1644669015	-1.9165046913
P	-0.0002405733	0.0247875833	1.0033437233
H	0.0001236412	-1.3900810571	0.8534957485

Frequencies

443.110
496.689
620.344
728.547
2172.667
2384.890

T1 diagnostic: 0.02293153

SiPH₂

P	-0.007083245	-7.651E-07	-0.952459448
Si	-0.007026817	1.0829E-06	1.206108617
H	0.611984756	1.088345885	-1.586755959
H	0.611984896	-1.088346175	-1.586758372

Frequencies

85.664
516.442
519.684
1099.794
2476.686

2489.275

T1 diagnostic: 0.02201284

t-HSiPH

Si	-0.001121064	0.059656434	-1.051034566
H	0.000054053	-1.201548382	-1.845544528
P	0.001550997	-0.0698775	1.006678943
H	-0.000432688	1.336709242	1.167899985

Frequencies

486.108
517.489
618.941
799.884
2184.361
2425.324

T1 diagnostic: 0.02926840

H2SiP

Si	-4.53118E-05	3.2107E-06	-1.016439058
P	0.000308946	-4.0339E-06	1.034078961
H	-0.00018872	1.218996045	-1.847328757
H	-0.000188757	-1.218995172	-1.847321565

Frequencies

470.927
532.046
637.480
951.198
2270.951
2289.755

T1 diagnostic: 0.01923710

Intermediates

S₁: SiPH₃; C_s; ¹A'

P	-0.0319137525	0.1448434866	-1.0514660901
Si	-0.1013182048	-0.2617615912	1.1358582412
H	-1.0653967923	0.5710264446	-1.9254211011
H	1.0453655690	0.6080548866	-1.8505414284
H	0.0032659206	-1.2305106665	-1.3525451615

Frequencies

307.059
440.759
518.405
904.242
991.556
1215.366
2315.492
2377.155
2481.575

T1 diagnostic: 0.01903879

T₁: SiPH₃; C_s; ³A''

P	-0.0165255199	-0.0000079012	-1.0183490506
Si	0.0097643708	0.0000033416	1.2767392804
H	1.2019260084	0.0000082112	-1.7266374244
H	-0.6374209112	-1.0624130355	-1.7054938117
H	-0.6374092854	1.0624093840	-1.7054896972

Frequencies

349.796
433.897
436.340
1045.821
1112.464
1112.654
2438.551
2438.729
2449.768

T1 diagnostic: 0.01728985

T_{2c}: HSiPH₂;

P	-1.0176895655	0.0454924199	-0.0001767107
Si	1.2801854915	0.0238966169	-0.0004684907
H	-1.6414381375	-0.6419281666	1.0610148565
H	-1.6417060079	-0.6480900352	-1.0572071985
H	0.5583340894	-1.3725813751	0.0037738833

Frequencies

214.388
371.165
416.352
594.096
719.400
1100.885
1793.358
2435.502
2446.735

T1 diagnostic: 0.02677059

T_{2b}: HSiPH₂; C_s; ³A"

Si	-0.0677196653	-0.1126810737	-1.1842206615
P	-0.0254978580	0.0692834278	1.0473488382
H	1.3269181877	-0.3155169764	1.1919507665
H	0.9866172567	0.4616067166	-2.0543963752
H	0.2598596790	1.4535738557	1.0694854520

Frequencies

213.864
447.391
504.125
683.444
726.257
1110.483
2209.441
2428.843
2432.091

T1 diagnostic: 0.01993677

T_{2a}: HSiPH₂; C_s; ³A"

P	-0.0731841655	0.0002958151	-1.0437309182
Si	0.0666272805	-0.0003694353	1.1815660841
H	0.8490097075	1.0346233839	-1.3118941627
H	0.8474235771	-1.0353230377	-1.3123810336
H	-1.2356882694	0.0004292093	1.8876247257

Frequencies

234.933
450.841
525.444
677.358
729.121
1123.347
2222.398
2442.862
2445.477

T1 diagnostic: 0.02684615

S₂: HSiPH₂; C₁; ¹A

P	-0.0611302598	-0.0022466922	-1.0210012220
Si	0.0230950033	0.0508314562	1.1814841787
H	0.6157392084	1.1297506545	-1.4984142360
H	0.7609067573	-1.0236709519	-1.5202845471
H	-0.0376407214	-1.4595427092	1.1860358819

Frequencies

209.076
488.062
513.009
519.667
818.151
1107.689
2099.036
2491.272

2510.576

T1 diagnostic: 0.02064757

T_{3b}: H₂SiPH; C_s; ³A"

Si	0.0025982593	0.0005696574	-1.1600188502
P	-0.0305882913	-0.0008887138	1.0879954593
H	-0.6508317715	1.2063303851	-1.7202077210
H	-0.6453498246	-1.2074519571	-1.7217125067
H	-1.4486100918	-0.0043534916	1.1266611385

Frequencies

330.008
452.898
497.122
504.744
746.937
914.577
2221.540
2246.035
2400.879

T1 diagnostic: 0.01737763

T_{3a}: H₂SiPH; C_s; ³A"

Si	0.0532368543	-0.0330639038	-1.1498781380
P	-0.0527187511	0.0093103118	1.0941414970
H	-1.1189797476	-0.7564148381	-1.6969807562
H	0.0200355775	1.3495336165	-1.6828838274
H	1.1788111193	-0.6597644851	1.2865216373

Frequencies

273.475
453.755
527.275
554.559
746.773
927.669
2221.255

2241.750
2424.889

T1 diagnostic: 0.02023070

S₃: H₂SiPH; C_s; ¹A'

Si	-0.0004061624	-0.0006313767	-1.0335912507
P	-0.0011280030	0.0447444991	1.0224291721
H	-0.0011869734	1.2238955015	-1.8522254331
H	0.0008003725	-1.2083840326	-1.8778493892
H	0.0001479545	-1.3725789235	1.0204239941

Frequencies

471.271
540.246
619.442
630.834
758.777
972.929
2284.226
2307.183
2420.222

T1 diagnostic: 0.01789945

T₄: H₃SiP; C_s; ³A''

Si	0.0022993848	0.0000002809	-1.0949847963
P	-0.0067987780	-0.0000003970	1.1480136847
H	1.3933100351	-0.0000001075	-1.5939684279
H	-0.6896908391	-1.2029612801	-1.6032729693
H	-0.6896910941	1.2029615037	-1.6032737686

Frequencies

459.281
505.540
505.663
909.236
950.620
950.818

2260.417
2267.789
2267.917

T1 diagnostic: 0.01351617

Transition states

T₁ - HPSi

P	-0.6408224232	0.1096626883	-0.8801031204
Si	0.2215050556	-0.1950568580	1.2644639802
H	0.7992402822	0.3248791818	-1.4946643314
H	-0.5615448008	-1.0708032896	-1.6560710735
H	0.1817042527	0.8307306117	-2.0109084228

Frequencies

-1274.405
168.716
350.855
437.966
933.090
1078.274
1779.341
2152.651
2404.554

T1 diagnostic: 0.02197400

S₁ - HPSi

P	0.0172259844	-0.0624066249	-0.9050676372
Si	-0.0099881102	0.0134348811	1.2075147596
H	0.5482766727	1.0949620991	-1.7903234554
H	0.0589225704	-0.9059752884	-2.0284611778
H	-0.5079397383	1.0787819497	-1.8152346708

Frequencies

-1516.106
72.037
395.410
528.344
951.764
1167.122
1743.381
1957.749
2437.445

T1 diagnostic: 0.02341995

T₁ - T₂

P	0.0135894813	0.0007288556	-1.1000971427
Si	0.0473650644	-0.0013928628	1.4571309106
H	-0.4622831724	1.0603258865	-1.8982482196
H	-0.4572824446	-1.0602658539	-1.8993780766
H	-1.1845791378	-0.0025482822	-0.2864676479

Frequencies

-498.878
198.018
267.153
989.052
1025.160
1125.663
2148.721
2450.122
2460.897

T1 diagnostic: 0.02039706

S₁ - S₂

P	-0.0354393643	0.1770926466	-1.0212779418
Si	-0.1025024120	-0.2794754928	1.0811259648
H	-1.0896230559	0.4498022001	-1.9375122683
H	1.0151796251	0.2050889941	-1.9792578463
H	0.2026597272	-1.2239863899	-0.7032858584

Frequencies

-717.054
446.533
542.704
567.439
1091.866
1239.970
2149.222
2294.277
2347.895

T1 diagnostic: 0.02335835

$T_1 - T_{2c}$

P	0.0135894813	0.0007288556	-1.1000971427
Si	0.0473650644	-0.0013928628	1.4571309106
H	-0.4622831724	1.0603258865	-1.8982482196
H	-0.4572824446	-1.0602658539	-1.8993780766
H	-1.1845791378	-0.0025482822	-0.2864676479

Frequencies

-498.878
198.018
267.153
989.052
1025.160
1125.663
2148.721
2450.122
2460.897

T1 diagnostic: 0.02039706

$T_{2c} - T_{2b}$

P	-1.1642105984	0.0825129775	-0.0007357653
Si	1.2598979478	-0.1526403032	-0.3197909676
H	-1.7253381877	-0.9107393651	0.8260214594
H	-1.8883978389	-0.3063452097	-1.1497406961

H 1.0557345471 -1.3059986395 0.6511823096

Frequencies

-900.460
197.817
266.050
455.423
473.141
1124.405
2023.588
2429.315
2467.545

T1 diagnostic: 0.02872943

T_{2a} - T_{2b}

P	0.0028989478	-0.4707063954	-1.4707362878
Si	0.1004855332	-0.6183794650	0.7848760314
H	-1.3836081778	-0.2024943127	-1.5328639465
H	0.3420289825	0.9027022432	-1.4272998604
H	1.0185797668	0.2984786313	1.4969444760

Frequencies

-253.278
439.984
511.355
640.877
749.793
1089.927
2229.197
2426.167
2433.875

T1 diagnostic: 0.02211549

T_{2a} - HPSi

P	-0.0001607814	-0.0067063495	-0.9915415515
Si	-0.0003129447	-0.0411138413	1.1528737468
H	-0.4000175078	1.7077467911	-1.6523653755

H	0.3996103564	1.7076763547	-1.6526331836
H	-0.0006108175	-1.4151090027	0.3748794609

Frequencies

-902.132
 222.177
 314.549
 517.134
 624.739
 771.411
 1032.008
 1816.478
 3484.438

T1 diagnostic: 0.04505358

T_{2a} - HSiP

P	-0.1284437991	0.0077950100	-1.0363960831
Si	0.0394655614	0.0448164674	1.0856929665
H	1.6326753762	0.2991827383	-1.4558543588
H	1.6168586273	-0.5013987640	-1.3494033143
H	-0.1420806977	-1.2163312098	1.8665088742

Frequencies

-847.465
 367.993
 444.200
 517.678
 564.471
 647.455
 1055.016
 2136.185
 3375.131

T1 diagnostic: 0.04664996

T_{2b} - T_{3b}

Si	-0.0670747137	-0.0691801973	-1.1675586565
P	-0.0232691989	0.0376075294	1.0775722595

H	1.3867569088	-0.0184094641	0.9258998757
H	1.2047188839	-0.0646081678	-1.9307964510
H	0.0213280371	1.2295534876	-0.1620733060

Frequencies

-1240.650
 269.397
 473.825
 510.160
 711.364
 932.901
 1638.483
 2209.852
 2405.228

T1 diagnostic: 0.02024202

T_{2a} - T_{3a}

Si	-0.0257841852	-0.0608539939	-1.1582883870
P	-0.0300675983	0.0580600638	1.0698437518
H	0.3281163090	-1.3004558846	1.2315102682
H	0.3607957506	1.2115622437	-1.8217692409
H	1.2290903432	-0.0341217194	-0.1101488796

Frequencies

-1052.019
 376.657
 468.472
 495.805
 799.182
 1009.292
 1656.753
 2198.416
 2429.637

T1 diagnostic: 0.02902485

S₂ - HSiP

P	0.8678158505	-0.2516991123	-0.0001225715
---	--------------	---------------	---------------

Si	-1.1867516146	-0.6561963965	0.0000778149
H	0.9711439536	1.6488223594	-0.3892226116
H	0.9702041470	1.6486788257	0.3891818126
H	-1.7161848667	0.7472746938	0.0000951256

Frequencies

-475.371
 223.953
 396.042
 474.476
 492.437
 607.214
 913.858
 2143.008
 3825.633

T1 diagnostic: 0.03715406

S₂ - HPSi

P	-0.0004128464	-0.0291300843	-1.2084145297
Si	-0.0001845846	0.0877309349	0.9059917306
H	-0.4079273329	1.6498635097	-1.4937158112
H	0.4075105112	1.6497620700	-1.4939241625
H	-0.0004774423	-1.4057324781	0.5212758698

Frequencies

-611.392
 338.261
 485.865
 637.434
 662.164
 806.706
 1371.016
 1957.360
 3328.625

T1 diagnostic: 0.02310587

S₂ - S₃

Si	-0.5404477827	-0.1968320542	-1.5587261521
P	-0.3832726562	0.2129469565	0.5535561048
H	0.3502128980	1.0189318187	-1.1393065493
H	0.3582603164	-1.3849414039	-1.6661015339
H	0.2134744445	-0.9630596572	1.0897651004

Frequencies

-1032.110
506.177
548.328
642.298
771.453
908.447
1842.297
2169.611
2375.443

T1 diagnostic: 0.03698734

T_{3a} - T_{3b}

Si	-0.0273397849	-0.3056984136	-1.2258086730
P	0.0354469405	-0.7416397876	1.0353561771
H	-1.4413433369	-0.3470881580	-1.6690017346
H	0.5001599544	1.0441716457	-1.5340043830
H	1.0134612793	0.2598554149	1.2443790261

Frequencies

-323.423
432.327
509.006
631.197
730.574
928.412
2219.802
2245.527
2428.618

T1 diagnostic: 0.01629213

T_{3b} - HPSi

Si	0.1051473113	0.0056961911	-1.1720144869
P	-0.0085922354	-0.0411628736	1.1005686201
H	-1.3449023339	0.3950801246	-1.6200317725
H	-1.3928986258	-0.5710479139	-0.9294457129
H	-0.1894708433	1.3681064306	1.1281438187

Frequencies

-1452.023
246.527
384.815
422.616
548.614
805.211
1686.320
1855.414
2383.860

T1 diagnostic: 0.02033087

T_{3a} - HPSi

Si	-0.0984719308	0.0189529704	-1.1662709024
P	0.0135000975	-0.0464395284	1.0980139048
H	1.3957263462	0.5196178091	-0.7647620383
H	1.3965943552	-0.3861236172	-1.4554352142
H	-0.1649281569	1.3377712484	1.3325616421

Frequencies

-1413.407
221.464
416.058
458.541
561.465
819.024
1714.267
1861.564
2416.519

T1 diagnostic: 0.02489786

T_{3b} - HSiP

Si	0.3831457471	0.7854519969	0.1237675148
P	-0.3725278044	-0.4796825338	1.8770570875
H	0.2649141446	-0.2803845779	-0.9297619649
H	1.2936919840	-0.3571002187	0.9335964695
H	1.8948779287	0.3317153332	0.4653408929

Frequencies

-1513.298
380.179
505.342
677.625
862.817
949.204
1675.218
1855.239
2122.361

T1 diagnostic: 0.02740054

S₃ - HSiP

Si	0.2515551522	0.3133796636	0.2057124214
P	-0.4377562872	-0.3197191671	1.9953493145
H	0.2686455486	0.0027920609	-1.2411821701
H	1.4748400260	-0.2847938359	1.0871343139
H	1.9068175604	0.2883412782	0.4229861202

Frequencies

-1565.546
290.452
542.453
644.155
781.396
1031.392
1750.143
1907.974
2233.235

T1 diagnostic: 0.02420061

S₃ - HPSi

Si	-0.0002326329	-0.7093912084	-1.2592534446
P	0.0003832199	0.1933494499	0.6366837223
H	-0.0003993490	0.8579267541	-1.6203633758
H	0.0003922983	-0.1248508856	-2.6409434942
H	-0.0001435361	-1.0950096514	1.2384929028

Frequencies

-1077.145
336.816
371.988
578.052
658.036
843.802
1730.549
2169.100
2379.365

T1 diagnostic: 0.02154998

T_{3b} - T₄

Si	-0.0567137141	0.0004315182	-1.1209238398
P	0.0004602713	-0.0009408228	1.1083091499
H	-0.3559314285	1.2444437195	-1.8452818841
H	-0.3502157270	-1.2439459669	-1.8469882699
H	-1.2807896417	-0.0031407880	-0.0221753561

Frequencies

-1336.350
434.489
472.243
535.973
724.518
909.453
1633.425
2284.765
2315.076

T1 diagnostic: 0.02327160

T₄ - HSiP

Si	-0.6586660172	0.0534639733	-0.9312658011
P	0.2551515316	-0.0695276704	1.0914110930
H	0.8784699167	0.2315102379	-1.4510624018
H	-0.6416174060	-1.2262326691	-1.6773856678
H	0.1667443650	1.0101984582	-1.8089802422

Frequencies

-1284.797
312.418
454.774
504.818
772.671
972.836
1723.609
2057.062
2239.537

T1 diagnostic: 0.02097781

MSX

MSX₁

P	-0.0343198014	0.1525524625	-1.0338534459
Si	-0.0922627118	-0.2636508794	1.1066970529
H	-1.0682879195	0.4278534880	-1.9701845395
H	1.0444781295	0.4661776307	-1.9055342091
H	-0.0076076968	-1.2650327018	-1.0587248584

Frequencies (Effective Hessian)

472.65
537.23
743.42
909.83

1203.02
2274.26
2287.80
2411.49

T1 diagnostic (singlet): 0.01900436
T1 diagnostic (triplet): 0.01772607

MSX₂

P	0.0176021892	-0.0668076713	-0.9134402743
Si	-0.0095163405	0.0291155029	1.1946887314
H	0.5978586607	1.0588537656	-1.7393593119
H	0.0584242972	-0.9239055193	-2.0355744280
H	-0.5585688065	1.0404439221	-1.7698147174

Frequencies (Effective Hessian)

-115.89
441.69
552.66
971.60
1200.22
1918.74
1975.30
2364.12

T1 diagnostic (singlet): 0.02131358
T1 diagnostic (triplet): 0.01998028

References

- (1) Kaiser, R. I.; Maksyutenko, P.; Ennis, C.; Zhang, F.; Gu, X.; Krishtal, S. P.; Mebel, A. M.; Kostko, O.; Ahmed, M. Untangling the Chemical Evolution of Titan's Atmosphere and Surface—from Homogeneous to Heterogeneous Chemistry. *Faraday Discuss.* **2010**, *147*, 429-478.
- (2) Thomas, A. M.; Dangi, B. B.; Yang, T.; Kaiser, R. I.; Sun, B.-J.; Chou, T.-J.; Chang, A. H. H. A Crossed Molecular Beams Investigation of the Reactions of Atomic Silicon (Si^3P) with C_4H_6 Isomers (1,3-Butadiene, 1,2-Butadiene, and 1-Butyne). *Chem. Phys.* **2019**, *520*, 70-80.
- (3) Thomas, A. M.; Dangi, B. B.; Yang, T.; Kaiser, R. I.; Lin, L.; Chou, T.-J.; Chang, A. H. H. Are Nonadiabatic Reaction Dynamics the Key to Novel Organosilicon Molecules? The Silicon (Si^3P)–Dimethylacetylene ($\text{C}_4\text{H}_6(\text{X}^1\text{A}_{1g})$) System as a Case Study. *J. Phys. Chem. Lett.* **2018**, *9*, 3340-3347.
- (4) Brink, G. O. Electron Bombardment Molecular Beam Detector. *Rev. Sci. Instrum.* **1966**, *37*, 857-860.
- (5) Daly, N. R. Scintillation Type Mass Spectrometer Ion Detector. *Rev. Sci. Instrum.* **1960**, *31*, 264-267.
- (6) Weiss, P. S. The Reactions of Ground and Excited State Sodium Atoms with Hydrogen Halide Molecules. Ph. D. Dissertation Thesis, University of California, Berkeley, California, 1986.
- (7) Vernon, M. F. Molecular Beam Scattering. Ph. D. Dissertation Thesis, University of California, Berkeley, California, 1983.
- (8) Schmidt, M. W.; Baldrige, K. K.; Boatz, J. A.; Elbert, S. T.; Gordon, M. S.; Jensen, J. H.; Koseki, S.; Matsunaga, N.; Nguyen, K. A.; Su, S.; Windus, T. L.; Dupuis, M.; Montgomery, J. A. General Atomic and Molecular Electronic Structure System. *J. Comput. Chem.* **1993**, *14*, 1347-1363.
- (9) Werner, H.-J.; Knowles, P. J.; Knizia, G.; Manby, F. R.; Schütz, M.; Celani, P.; Györfly, W.; Kats, D.; Korona, T.; Lindh, R.; Mitrushenkov, A.; Rauhut, G.; Shamasundar, K. R.; Adler, T. B.; Amos, R. D.; Bernhardsson, A.; Berning, A.; Cooper, D. L.; Deegan, J. O.; Dobbyn, A. J.; Eckert, F.; Goll, E.; Hampel, C.; Hesselmann, A.; Hetzer, G.; Hrenar, T.; Jansen, G.; Köppl, C.; Liu, Y.; Lloyd, A. W.; Mata, R. A.; May, A. J.; McNicholas, S. J.; Meyer, W.; Mura, M. E.; Nicklass, A.; O'Neill, D. P.; Palmieri, P.; Peng, D.; Pflüger, K.; Pitzer, R.; Reiher, M.; Shiozaki, T.; Stoll, H.; Stone, A. J.; Tarroni, R.; Thorsteinsson, T.; Wang, M. *MOLPRO, Version 2015.1, A Package of Ab Initio Programs*. University of Cardiff: Cardiff, UK, 2015; <http://www.molpro.net>.
- (10) Kohn, W.; Sham, L. J. Self-consistent Equations including Exchange and Correlation Effects. *Phys. Rev.* **1965**, *140*, A1133.
- (11) Zhao, Y.; Truhlar, D. G. The M06 Suite of Density Functionals for Main Group Thermochemistry, Thermochemical kinetics, Noncovalent Interactions, Excited States, and Transition Elements: Two New Functionals and Systematic Testing of Four M06-Class Functionals and 12 Other Functionals. *Theor. Chem. Acc.* **2008**, *120*, 215-241.
- (12) Dunning Jr, T. H.; Peterson, K. A.; Wilson, A. K. Gaussian Basis Sets for Use in Correlated Molecular Calculations. X. The Atoms Aluminum through Argon Revisited. *J. Chem. Phys.* **2001**, *114*, 9244-9253.
- (13) Dunning Jr, T. H. Gaussian Basis Sets for Use in Correlated Molecular Calculations. I. the Atoms Boron through Neon and Hydrogen. *J. Chem. Phys.* **1989**, *90*, 1007-1023.

- (14) Kendall, R. A.; Dunning Jr, T. H.; Harrison, R. J. Electron Affinities of the First-row Atoms Revisited. Systematic Basis Sets and Wave Functions. *J. Chem. Phys.* **1992**, *96*, 6796-6806.
- (15) Peverati, R.; Truhlar, D. G. M11-L: A Local Density Functional that Provides Improved Accuracy for Electronic Structure Calculations in Chemistry and Physics. *J. Phys. Chem. Lett.* **2012**, *3*, 117-124.
- (16) Berkowitz, J.; Curtiss, L. A.; Gibson, S. T.; Greene, J. P.; Hillhouse, G. L.; Pople, J. A. Photoionization Mass Spectrometric Study and *Ab Initio* Calculations of Ionization and Bonding in P-H Compounds; Heats of Formation, Bond Energies, and the $^3B_1-^1A_1$ Separation in PH^+_2 . *J. Chem. Phys.* **1986**, *84*, 375-384.
- (17) Walsh, R. Bond Dissociation Energy Values in Silicon-Containing Compounds and Some of Their Implications. *Acc. Chem. Res.* **1981**, *14*, 246-252.
- (18) Koga, N.; Morokuma, K. Determination of the Lowest Energy Point on the Crossing Seam between Two Potential Surfaces using the Energy Gradient. *Chem. Phys. Lett.* **1985**, *119*, 371-374.
- (19) Harvey, J. N.; Aschi, M. Spin-forbidden Dehydrogenation of Methoxy Cation: a Statistical View. *Phys. Chem. Chem. Phys.* **1999**, *1*, 5555-5563.
- (20) Nunes, C. M.; Viegas, L. P.; Wood, S. A.; Roque, J. P. L.; McMahon, R. J.; Fausto, R. Heavy-Atom Tunneling Through Crossing Potential Energy Surfaces: Cyclization of a Triplet 2-Formylarylnitrene to a Singlet 2,1-Benzisoxazole. *Angew. Chem. Int. Ed.* **2020**, *59*, 17622-17627.
- (21) Gannon, K. L.; Blitz, M. A.; Liang, C.-H.; Pilling, M. J.; Seakins, P. W.; Glowacki, D. R.; Harvey, J. N. An Experimental and Theoretical Investigation of the Competition between Chemical Reaction and Relaxation for the Reactions of $^1\text{CH}_2$ with Acetylene and Ethene: Implications for the Chemistry of the Giant Planets. *Faraday Discuss.* **2010**, *147*, 173-188.
- (22) Berning, A.; Schweizer, M.; Werner, H.-J.; Knowles, P. J.; Palmieri, P. Spin-Orbit Matrix Elements for Internally Contracted Multireference Configuration Interaction Wavefunctions. *Mol. Phys.* **2000**, *98*, 1823-1833.
- (23) Adler, T. B.; Knizia, G.; Werner, H.-J. A Simple and Efficient CCSD(T)-F12 Approximation. *J. Chem. Phys.* **2007**, *127*, 221106.
- (24) Knizia, G.; Adler, T. B.; Werner, H.-J. Simplified CCSD(T)-F12 Methods: Theory and Benchmarks. *J. Chem. Phys.* **2009**, *130*, 054104.
- (25) Lee, T. J. Comparison of the T_1 and D_1 Diagnostics for Electronic Structure Theory: a New Definition for the Open-shell D_1 Diagnostic. *Chem. Phys. Lett.* **2003**, *372*, 362-367.